Inter-individual variability in the expression of the mutated form of hPS1M146L determined the production of Abeta peptides in the PS1xAPP transgenic mice

Cristina Caballero [1], Sebastian Jimenez [1], Ines Moreno-Gonzalez [2], David Baglietto-Vargas [2], Raquel Sanchez-Varo [2], Mari Paz Gavilan [1], Blanca Ramos [1], Juan Carlos del Rio [1], Marisa Vizuete [2], Antonia Gutierrez [2], Diego Ruano [1], Javier Vitorica [1]

Affiliations:

[1]Departmento de Bioquímica, Bromatologia, Toxicología y Medicina Legal, Facultad de Farmacia, Universidad de Sevilla, 41012 Sevilla, Spain

[2]Departmento Biología Celular, Genética y Fisiología, Facultad de Ciencias, Universidad de Malaga, Malaga, Spain

Cristina Caballero and Sebastian Jimenez contributed equally to this article

* Corresponding Author:

Javier Vitorica
Dept. Bioquímica, Bromatología, Toxicología y Medicina Legal
Facultad de Farmacia, Universidad de Sevilla
c/Prof. Garcia Gonzalez 2
41012, Sevilla, España
Fax: +34 952233765
Email: vitorica@us.es

Keywords: Alzheimer; transgenic; Aβ; heterogeneity; PS1; γ-secretase

Abstract

The detection of the early phenotypic modifications of Alzheimer's disease (AD) models is fundamental to understand the progression and identify pharmacologic targets of this pathology. However, a large variability within different models and between age-matched mice from the same model has been observed. This variability could be due to heterogeneity in the Aβ production. Present results showed the existence of a large variability in the Aβ deposition in both hippocampus and cortex in 6-month-old PS1xAPP mice. This variability was not due to the expression of hAPP751SL, however, linear relationship between hPS1M146L mRNA and Aβ production was identified. The Aβ content was related to the incorporation of the hPS1M146L into functional γ-secretase complexes, detected by the presence of the corresponding human or endogenous PS1-CTFs. Animals expressing low amount of hPS1M146L mRNA, displayed low hPS1-CTF incorporation and produced a low amount of Aβ peptides. Conversely, mice with relatively high hPS1 mRNA expression displayed high hPS1-CTF and high Aβ deposition. Furthermore, the Aβ total and Aβ1-42 content was increased dramatically by the expression of hPS1M146L (as compared with transgenic APPsl littermates). Therefore, variations in the expression of transgenic form of hPS1M146L in this model, or even between different models, influenced strongly the incorporation of the mutated PS1 into functional γ-secretase complexes, the production of Aβ peptides and, in consequence, the detrimental effects of Aβ peptides. These data might implicate an "apparent gain-of-function" of the γ-secretase complex by the expression of the mutated PS1M146L.

Alzheimer's disease (AD) is a devastating neurodegenerative disorder affecting predominantly individuals over age of 65. The neuropathologic lesions of AD are the presence of beta amyloid (Aβ) deposits and plaques, hyperphosphorylation of τ, and neurofibrillary tangles and degeneration of synapses together with neuronal cell loss (West et al., 1994, 2004; Price et al., 1998; Selkoe, 2002). At present, however, no effective pharmacologic treatment has been developed against this irreversible degenerative process. The lack in therapeutic treatment is due, at least in part, to the absence of animal models that mimic the neuropathologic progression of this disorder. In this sense, a relative high number of genetically modified mice have been developed as valuable tools of AD. Most AD models have been designed to mimic the Aβ depositions observed in patients because compelling evidence indicates the Aβ neurotoxicity as the principal cause of all AD cases (Hardy and Selkoe, 2002). These transgenic (tg) mice reproduced most, but not all, aspects of AD.

The phenotypic characterization of the different AD models is a preliminary, but relevant, goal in the study of the AD progression, the identification of new therapeutic targets, and the development of new pharmacologic approaches against this devastating illness. In this sense, using a PS1M146L (hPS1) x APP751SL (hAPP) transgenic (tg) model developed previously (Blanchard et al., 2003; Schmitz et al., 2004), we have reported recently the existence of an early neurodegenerative process affecting specifically a subset of hippocampal neurons of the GABAergic system in a PS1xAPP tg mice (Ramos et al., 2006). Our results also showed the existence of high variability among mice within the same age group (Ramos et al., 2006). This inter-individual variability was observed predominantly at early ages (4–6-month-old), when the initial neurodegenerative process should take place. In consequence, the existence of such variability could obscure the results and conclusions achieved from these models. Because most tg models are based on the overproduction of Aβ peptides, the observed variability could derive from, among other reasons, inter-individual variations in the Aβ production. We have addressed this problem by determining the Aβ content and the expression of proteins implicated in the synthesis and degradation of the Aβ peptides in cortex and hippocampus of 6-month-old PS1xAPP tg mice. Our results showed that the variable content of Aβ peptides within the different tg mice could reflect the variable insertion of the hPS1M146L subunit into the γ-secretase complexes. Furthermore, these data could be interpreted as an "apparent gain-of-function" of the γ-secretase due to the presence of the mutated PS1 form.

Materials and methods

Transgenic Mice

The generation and initial characterization of the PS1 and PS1xAPP tg mice has been reported previously (Blanchard et al., 2003). PS1 tg mice (C57BL/6 background) overexpressed the mutated hPS1M146L form under the control of the HMGCoA-reductase promoter. PS1xAPP double tg mice (C57BL/6 background) were obtained by crossing homozygotic PS1 tg mice with heterozygotic Thy1-APP751SL mice (Transgenic Alliance, Lyon, France). Mice represented F6–F10 offspring of heterozygous tg mice. Non-transgenic mice of the same genetic background were used as controls. Anesthetized male mice were sacrificed by decapitation and both hippocampi and cortex

were dissected, frozen in liquid N_2, and stored at −80°C until use. All animal experiments were carried out in accordance with the NIH Guide for the care and use of laboratory animals and the guidelines of the Committee on Animal Research of the University of Seville.

RNA and Protein Extraction

Total RNA and proteins were extracted using the TripureTM Isolation Reagent (Roche, Mannheim, Germany), according to the instructions of the manufacturer. This procedure allows the isolation of total RNA, DNA and protein fractions from a single sample. The contaminating DNA in the RNA samples was removed by incubation with DNAase (Sigma-Aldrich, St. Louis, MO) and confirmed by PCR analysis of total RNA samples before reverse transcription (RT). After isolation, the integrity of the RNA samples was assessed by agarose gel electrophoresis. The yield of total RNA was determined by measuring the absorbance (260/280 nm) of ethanol precipitated aliquots of the samples. The recovery of RNA was comparable in all groups (1.2–1.5 μg/mg of tissue).

To analyze the protein fraction, the protein pellets obtained using the Tripure Isolation Reagent were resuspended in 4% SDS and 8 M urea in 40 mM Tris-HCl, pH 7.4 and rotated overnight at room temperature. The total recovery and integrity of these fractions were determined by Lowry et al. (1951) and SDS-PAGE.

Real-Time PCR

The retrotranscription (RT) was done using random hexamers, 4 μg of total RNA as template, and Ready-To-Go You-Prime First-Strand Beads (Amersham, GE Healthcare, Barcelona, Spain) or High-Capacity cDNA Archive Kit (Applied Biosystems, Foster City, CA) following the manufacturer's recommendations. After RT, the cDNA was purified using Microcon PCR cartridges (Millipore) and quantified by measuring the absorbance at 260/280 nm. For real time RT-PCR, each specific gene product was amplified using commercial Taqman probes, following the instructions of the manufacturer (Applied Biosystems), using an ABI Prism 7000 sequence detector (Applied Biosystems). For each assay, a standard curve was constructed using increasing amounts of cDNA. In all cases, the slope of the curves indicated adequate PCR conditions (slope = 3.2–3.4). The cDNA levels of the different mice were determined using two different housekeepers (i.e., GAPDH and β-actin). The amplification of the housekeepers was done in parallel with the gene to be analyzed. Similar results were obtained using both housekeepers. Thus, the results were normalized using only the GAPDH expression.

Western Blot

Western blots were carried out as described previously (Araujo et al., 1996). Briefly, for Aβ detection, a total of 2.5 μg of hippocampal proteins were loaded onto a 16% SDS-Tricine. For C99 and PS1 CTF detection, a total of 2.5 μg or 20 μg, respectively, of hippocampal proteins were loaded onto a linear 4–20% acrylamide gradient (Bio-Rad). After transference to a nitrocellulose (Hybond-C Extra, Amersham, Sweden) the membranes were blocked and incubated overnight at 4°C with the following primary antibodies: 1) for Aβ detection, monoclonal 6E10 (Sigma-Aldrich; dilution 1/2000); 2)

for C99, polyclonal anti-APP C-terminal peptide (Sigma-Aldrich; dilution 1/4,000); and 3) for PS1-CTF, monoclonal MAB5232 (Chemicon; dilution 1/2000). In all cases, the protein loading was tested using a monoclonal anti β-actin (Sigma-Aldrich; dilution 1/4,000). The membranes were incubated with either anti-mouse (1/4,000) or anti-rabbit (1/6,000) horseradish-peroxidase-conjugated secondary antibody (Dako, Denmark). The blots were developed using the ECL-plus detection method (Amersham, Sweden).

Co-Immunoprecipitation

The co-immunoprecipitation experiments were done essentially as described previously (Araujo et al., 1996). Briefly, the membranes were solubilized at 2 mg of protein/ml using 1% (w/v) CHAPSO in 150 mM NaCL, 1 mM EDTA, 1 mM EGTA, 10 mM tris-HCl, pH 7.4, and complete protease inhibitor cocktail (Sigma-Aldrich). After solubilization, 50–100 μg proteins were subjected to immunoprecipitation by overnight incubation (at 4°C) in anti-nicastrin-protein A-sepharose slurry. The immunoprecipitates were washed with the solubilization buffer, eluted using Laemli dissociation buffer and analyzed by Western blot using anti-PS1-CTF (MAB5232, Chemicon).

Tissue Preparation

After deep anesthesia with sodium pentobarbital (60 mg/kg), 6-month-old PS1xAPP tg mice (n = 7) were perfused transcardially with 0.1 M phosphate-buffered saline (PBS), pH 7.4 followed by 4% paraformaldehyde, 75 mM lysine, 10 mM sodium metaperiodate in 0.1 M phosphate buffer (PB), pH 7.4. Brains were then removed, post-fixed overnight in the same fixative at 4°C, cryoprotected in 30% sucrose, sectioned at 40 μm thickness in the coronal plane on a freezing microtome, and serially collected in wells containing cold PBS and 0.02% sodium azide. All animal experiments were carried out in accordance with the NIH Guide for the Care and Use of Laboratory Animals and approved by the Committee of Animal Use for Research at Malaga University.

Sections that represented one-seventh of the total hippocampus from each 6-month-old PS1xAPP tg mice were processed in parallel for light microscopy immunostaining using the same batches of solutions to minimize variability in immunocytochemical labeling conditions. Free-floating sections were first treated with 3% H_2O_2/3% methanol in PBS, pH 7.4 for 15 min to inhibit endogenous peroxidases, and with avidin-biotin Blocking Kit (Vector Labs, Burlingame, CA) for 30 min to block endogenous avidin, biotin, and biotin-binding proteins. Sections were then immunoreacted with anti-Aβ monoclonal antibody 6E10 (1:1,500 dilution; Sigma) overnight at room temperature. The tissue-bound primary antibody was then detected by incubating for 1 hr with goat anti-mouse biotinylated secondary antibody (1:500 dilution, Vector Laboratories), and then followed by incubating for 90 min with streptavidin-conjugated horseradish peroxidase (1:2,000 dilution, Sigma). Peroxidase reaction was visualized with 0.05% 3-3′-diaminobenzidine tetrahydrochloride (DAB; Sigma), 0.03% nickel ammonium sulphate, and 0.01% hydrogen peroxide in PBS. Sections were mounted on gelatin-coated slides, air dried, dehydrated in graded ethanols, cleared in xylene, and coverslipped with DPX (BDH) mounting medium. Specificity of the immunoreaction was controlled by omitting the primary antibody.

Plaque Loading Quantification

Hippocampal 6E10 immunostaining was observed under a Nikon Eclipse 50i microscope using a 4× objective and images acquired with a Nikon DS-5M high-resolution digital camera. The camera settings were adjusted at the start of the experiment and maintained for uniformity. Digital images (seven sections/mouse from seven different 6-month-old APPxPS1 mice) were analyzed using Visilog 6.3 analysis program (Noesis, France). The plaque area within the hippocampus was identified by bright-level threshold, the level of which was maintained throughout the experiment for uniformity. The gray-scale image was converted to a binary image with plaque and hippocampal field areas identified. Plaque loading was defined as percentage of total hippocampal area stained for Aβ, excluding principal cell layers intracellular labelling that was removed by manual editing. The hippocampal area in each 4× image was manually outlined. The plaque loading (%) for each tg mouse was estimated and defined as (sum plaque area measured/sum hippocampal area analyzed) × 100. The sums were taken over all slides sampled and a single plaque burden was computed for each mouse. The mean and standard deviation (SD) of the plaque loading were determined using all the available data. Quantitative comparisons were carried out on sections processed at the same time.

ELISA Assays

The Aβ total and Aβ42, from 9 M guanidine HCl extracted samples, were determined by electrochemiluminiscence sandwich ELISA using ruthenylated 4G8 monoclonal antibody. The monoclonal 6E10 or the monoclonal 22F9, for Aβ total or Aβ42, respectively, were used as capture antibodies (Blanchard et al., 2003).

Statistical Analysis

Data were expressed individually or as mean ± SD. For RT-PCR real time quantification the individual data are mean of at least two different experiments. The Western blots were repeated three times. The comparison between two mice groups (APP and PS1APP tg mice) was done by two-tailed *t*-test (Statgraphics +3.1). The significance was set at 95% of confidence.

Results

Heterogeneity in the Aβ Production

The Aβ production was first determined by Western blots using the mAb 6E10, in hippocampus and cortex of 6-month-old PS1xAPP tg mice. As shown in Figure 1A,B, a 4.5 kDa immunostained band (corresponding to the monomeric form of Aβ, as compared with synthetic Aβ peptides (Walsh et al., 2002), was observed clearly in both brain areas. As also shown (Fig. 1A,B), the Aβ content in the PS1xAPP tg mice displayed high inter-individual heterogeneity (Ramos et al., 2006). This heterogeneity was not due to differences in the original protein loading, as probed by re-incubating the same Western blots with anti β-actin (Fig. 1A,B, lower panel). This heterogeneous profile was observed quantitatively in both brain regions tested (Fig. 1C). A significant linear correlation could be established between the Aβ content detected in hippocampus and cortex (Fig. 1D),

indicating that the high inter-individual variability in the Aβ production was an intrinsic property of this tg model. Using ELISA (Blanchard et al., 2003) a similar heterogeneity in both, the total Aβ and Aβ1-42 was also observed in the hippocampal samples (Fig. 1E).

We have also tested by immunohistochemistry, using the mAb 6E10, whether the variability in the Aβ production was also reflected in the extracellular deposition of Aβ in the hippocampus. As shown in Figure 1F, in 6-month-old PS1xAPP tg mice, multiple Aβ depositions were observed at all hippocampal subfields (CA1–3) and dentate gyrus. The amount of extracellular Aβ deposits in the hippocampus was significantly different among animals at this age for a tg mice with high Aβ production (Fig. 1, upper panel) and another with low production (Fig. 1, lower panel). The percent area occupied by Aβ-immunoreactive plaques was used to estimate the amyloid load in the hippocampus of seven different tg mice (Fig. 1G). Within this age group, the percentage of area covered by Aβ deposits in the hippocampus was also highly variable (i.e., 7.2 times between the higher and lowest Aβ produced age-matched mice).

The inter-individual variability could be due, among other factors, to differences in the expression of the Aβ degrading or synthesizing enzymes. We have quantitatively determined the expression of the mRNAs coding for BACE1, IDE, and neprilysin (Iwata et al., 2001; Leissring et al., 2003) in the cortex and hippocampus of 6-month-old WT and PS1xAPP tg mice. The results (not shown) indicated the absence of differences between WT and PS1xAPP mice in the IDE and BACE1 mRNA expression whereas the neprilysin expression increased significantly in hippocampus and cortex from PS1xAPP tg mice. This increase agreed with the role of the intracellular domain of APP in the transcriptional control of neprilysin (Pardossi-Piquard et al., 2005). However, no apparent relationship between the Aβ production and the expression levels of any of the three mRNAs was observed (not shown). It is unlikely that the inter-individual variability in the Aβ production was due to differences in the expression of IDE, neprilysin, or BACE1.

The Variable Expression of hPS1 Modulated the Accumulation of Aβ Peptides

Next, we tested whether the observed variability in the Aβ production was due to differences in the content of full length APP or in the corresponding C99 fragment in the hippocampus. As shown in Figure 2A–C, no major inter-individual differences were observed in either full length APP or C99 fragments, as compared with the Aβ production (Fig. 2C).

These results prompted us to investigate the expression of the transgenic hAPP and hPS1 mRNAs in the same WT and PS1xAPP populations. As expected, no expression of hAPP or hPS1 was detected in WT mice (not shown) whereas the expression of hAPP mRNA was high in both brain areas (Fig. 2D) and similar within the different PS1xAPP mice tested. On the contrary, the expression levels of the mRNAs coding for hPS1 displayed an unexpected high variability in our tg population (Fig. 2D). This variability was very similar to that observed for the Aβ production. To verify the existence of such variability in the hPS1 expression we have extended our analysis to hippocampus and cortex from 4- and 12-month-old PS1xAPP tg mice. The results (not shown) showed: 1) that the expression levels did not change with age, and 2) a similar heterogeneity was observed at

all ages and in both brain areas. Similar to the Aβ content, there was a highly significant linear correlation between the hPS1 expression in hippocampus and cortex (Fig. 2E).

These data suggested that variations in the expression of the tg hPS1 could be implicated in the different Aβ production of the PS1xAPP population. To test this proposal, we have plotted the hPS1 mRNA expression levels versus the Aβ content form both hippocampus and cortex of 6-month-old PS1xAPP tg mice. There was a significant linear correlation between the expression of hPS1 and the production of Aβ peptides in both hippocampus and cortex (Fig. 2F). A similar linear correlation was also observed in 4- and 12-month-old tg mice (not shown).

The existence of this correlation between hPS1 mRNA and Aβ content suggested that the hPS1 expression could be the limiting factor in the Aβ production by the γ-secretase complex. However, among other factors, the γ-secretase activity was regulated by the assembling of the different components of this complex (Nicastrin, Pen2, and Aph1), not only by the expression of a single subunit (Edbauer et al., 2003; Kimberly, 2003). It was also known that the PS1 protein was cleaved into N- and C-terminal fragments after its insertion into functional γ-secretase complexes (Thinakaran et al., 1996). Thus, we next evaluated whether the heterogeneity in the hPS1 mRNA expression was also reflected in the hPS1 assembled into functional γ-secretase complexes by analyzing the C-terminal fragment of the PS1 subunit. We used the protein samples from hippocampus of the same 6-month-old WT and PS1xAPP mice as before. As shown in Figure 3A, in WT mice the endogenous PS1-CTF was observed as a single band of Mr 20 kDa whereas the CTF corresponding to the transgenic hPS1 displayed a slightly higher Mr (see lanes 2, 3, 5, and 6 in Fig. 5A) (Thinakaran et al., 1996). Also shown in Figure 3A, the relative amount of human PS1-CTF displayed high heterogeneity within the different 6-month-old PS1xAPP mice tested. The results showed clearly that some PS1xAPP tg mice displayed very low levels of hPS1 CTF (e.g., no. 15, Fig. 3A, lane 5). These animals also showed very low amount of Aβ production (Fig. 1) and low levels of hPS1 mRNA. Conversely, in other age-matched tg animals most of the detected PS1-CTF corresponded to the human variant (e.g., no. 233, lane 6). Consequently, the Aβ production in these tg mice was elevated (Fig. 1). These data indicated strongly that the insertion of the hPS1 variant into the γ-secretase complex could increase the Aβ production. In fact, there was a significant linear correlation between the Aβ content and the relative hPS1-CTF expression in both hippocampus (Fig. 3B) and cortex (not shown) of 6-month-old PS1xAPP tg mice. The total amount of PS1-CTF (hCTF + mCTF) increased only slightly in the PS1xAPP tg mice (as compared with WT) and displayed a clear saturation plateau (Lee et al., 1997; Borchelt et al., 2002) (Fig. 3). The total PS1-CTF presented in the double tg mice represented 165 ± 49% (n = 11), as compared with WT mice. The absence or small repercussion of the tg hPS1M146L overexpression in the total γ-secretase complex was also assessed by quantifying the total PS1-CTFs (murine + human) co-immunoprecipitated with nicastrin, in WT and PS1xAPP tg mice (Fig. 3E). After solubilization (using CHAPSO), it was not possible to discriminate between the human and the murine PS1 isoforms in the solubilized fraction (Fig. 3E, solubilized membranes) or in the remaining pellets (not shown). Thus, we have quantified the total PS1-CTF co-immunopreciptated by nicastrin from WT and PS1xAPP tg mice. As shown in Figure 3F, after normalization by the signal observed in WT mice, the PS1-CTF co-

immunoprecipitated from PS1xAPP tg mice represented a small and no significant increase (1.0 ± 0.15 vs. 1.27 ± 0.36, n = 6, for WT and PS1xAPP, respectively).

These data could be explained if the hPS1 competes with the mPS1 for the insertion into the gamma secretase complex. As shown in Figure 3D, this seems to be the case. At relative low levels of hPS1-CTF expression, the corresponding endogenous PS1-CTF was unaffected. Only those tg mice displaying high hPS1 mRNA expression (that corresponded to high hPS1-CTF and Aβ production) also showed a reduction in the murine PS1-CTF. However, no accumulation of full length PS1 was detected in any of the WT or PS1xAPP mice tested (not shown).

These data showed that the variable levels in the expression of the mutant hPS1 determined the variable insertion of the corresponding hPS1 subunit into the γ-secretase complex and, in consequence, the variable production of Aβ peptides in the different PS1xAPP tg mice. In consequence, the presence of the mutated hPS1M146L subunit into the γ-secretase complex should increase the production of Aβ peptides. To test this proposal, we crossed hemizygous PS1M146L with hemizygous APPsl tg mice. All four genotypes (WT, PS1, APP, and PS1xAPP) were obtained in the first generation. We tested (by ELISA) the total and 1-42 Aβ peptides from hippocampus and cortex extracted with guanidine HCl (Blanchard et al., 2003). Results are shown in Figure 4. No Aβ peptides could be detected in either WT or PS1 tg mice at this age (6-month-old, not shown). As expected from previous data using this tg model, the amounts of both total and 1-42 peptides increased significantly in PS1xAPP tg mice, as compared with APP littermates. In fact, the production of total Aβ by PS1xAPP mice increased 5.9 ± 1.9 folds (n = 7 as compared with APP littermates) in both hippocampus and cortex. Interestingly, the increase in the Aβ42 production was even higher (11.5–14.1-fold). In consequence, there was also an increase in the Aβ42/Aβ total ratio (Fig. 4). No apparent modifications on the hAPPsl mRNA expression between APP and PS1xAPP littermates were detected (not shown).

Discussion

The phenotypic characterization of the different AD models is a preliminary, but relevant, goal in the study of the AD progression, the identification of new therapeutic targets, and the development of new pharmacologic approaches against this devastating illness. Using this PS1xAPP tg model, we have reported recently the existence of an early and heterogeneous neurodegenerative process affecting specifically to the hippocampal somatostatin/NPY interneurons (Ramos et al., 2006). An inverse linear correlation could be established between the Aβ accumulation and the somatostatin or NPY expression on the different age-matched PS1xAPP tg mice. We have investigated the origin of the observed variability in the Aβ production by our tg model.

Results showed that the heterogeneous production of Aβ peptides reflected the different expression of the transgenic variant hPS1M146L subunit in the different tg individuals. Considering that the endoproteolysis of PS1 might reflect the incorporation of the PS1 into functional γ-secretase complexes (Thinakaran et al., 1996; Li et al., 2000; Campbell et al., 2002), the correlation between hPS11M146L mRNA levels and the Aβ content in

cortex and hippocampus and, more relevant, the Western blot analysis of the murine and human PS1-CTFs, strongly supported this conclusion. Considering we have not determined directly the incorporation of hPS1M146L into mature γ-secretase complexes, our results showed that the Aβ content was clearly related to the presence of the corresponding human or endogenous PS1-CTFs. As expected, animals expressing low amounts of tg hPS1 mRNA, displayed low hPS1-CTF incorporation and, in consequence, produced low amounts of Aβ peptides. Conversely, mice with relatively high hPS1 mRNA expression displayed high hPS1-CTF and high Aβ deposition. Therefore, these data indicated that variations in the expression of tg form of the hPS1 strongly influenced the incorporation of the mutated hPS1 into functional γ-secretase complexes, the production of Aβ peptides and, in consequence, the detrimental effects of the production of Aβ peptides. These results are apparently in conflict with those reported by others (Borchelt et al., 2002). This apparent discrepancy could be due to differences in hPS1 expression between our tg model and those reported previously in other tg models. In our case, the detected levels of hPS1-CTF were in the same range of the WT counterpart (Fig. 3A). Even in the low hPS1 expressing tg mice from Borchelt et al. (2002) the hPS1-CTF was considerable higher than that present in WT mice. The high expression of hPS1 protein observed in other tg models could saturate the assembling process of the γ-secretase complex and, in consequence, the hPS1 incorporated into the complexes should be independent of the mRNA expression. However, in our tg model (as well as in other tg models) (Lewis et al., 2004), the relatively low levels of hPS1 protein determined the competition with the endogenous subunit (Fig. 3D) and, in consequence, an increase in the hPS1 expression might also be reflected by an increase in the incorporation of hPS1 subunit in the γ-secretase.

Our results also showed that the presence of the PS1M146L tg increased dramatically the production of Aβ (total and 1-42) and the ratio Aβ42/Aβ total. This latter effect has been consistently reported in several in vivo and in vitro models. However, the effect of the FAD mutations on the γ-secretase activity was conflictive. In this sense, several recent in vitro and in vivo experiments have shown consistently that the FAD mutations produced a reduction on the γ-secretase activity (Wang et al., 2006). Our results, however, did not support this conclusion. As shown in Figure 4, the production of both Aβ total and Aβ1-42, was enhanced highly in PS1xAPP double tg mice, as compared with APP littermates. This increase in the Aβ (total and 1-42) production in the double tg mice, detected by ELISA, was internally consistent with the observed increase in the Aβ production, detected by Western blots, in correlation with the hPS1 expression of the different tg mice.

It could be argued that the enhanced Aβ production in the PS1xAPP mice, was reflecting an increase in the total γ-secretase complex due to the overexpression of the tg hPS1 isoform. However, this explanation seems unlikely. As also shown by our data, the total PS1-CTF (human + murine, determined by Western blots) in the tg mice represented 165 ± 49% of the WT mice. Furthermore, this small increase in the total PS1-CTF was also supported by the co-immunprecipitation experiments (127 ± 36% of WT mice). This increase could not explain the dramatic increment in the total and Aβ1-42 production. In consequence, the increase in the Aβ production could not be explained exclusively by an increase in the total γ-secretase activity due to the presence of the transgenic hPS1. These

data were compatible with the existence of an "apparent gain-of-function" of the γ-secretase complex by the presence of the tg PS1M146L subunit. It could be also argued, however, that the increase in the Aβ production was due to the transgenic expression of the human PS1 isoform and unrelated to the presence of the M146L mutation. Because the proper control model, WT hPS1xAPPsl tg mice, is not available presently, we cannot answer this question directly. However, in a similar PS1xAPP tg model (Dewachter et al., 2000) only the presence of the mutant (A246E), but not the WT hPS1, increased the brain Aβ levels and the amyloid plaque formation. Furthermore, indirect evidences also indicated the absence of major repercussion in the overexpression of WT hPS1 in either the transcriptome from hippocampus and frontal cortex (Mirnick et al., 2005; Unger et al., 2005) or in the unfolding protein response (Terro et al., 2002). We cannot discard this possibility completely.

It is difficult to reconcile the increase in the Aβ production (our data; see also Blanchard et al., 2003) with the observed decrease in the γ-secretase activity induced by FAD mutations. It is possible that the particular FAD mutation used in our tg model (PS1M146L) could directly produce a gain-of-function in the γ-secretase complex, although in vitro assays did not support this fact (Kakuda et al., 2006). Alternatively, it is also plausible that the PS1 subunit directly, or in conjunction with other components of the complex, could exert other functions related to the Aβ metabolism, such as influencing the activity of Aβ degrading enzymes (Pardossi-Piquard et al., 2005) or even modulating the γ-secretase activity (Cai et al., 2006; Chen et al., 2006). The existence of additional proteins in the γ-secretase complex or additional functions of the PS1 subunit has been proposed (Chen et al., 2006; Doglio et al., 2006). It is tempting to speculate that the same FAD mutations that decreased the γ-secretase activity could also influence negatively the modulation of the γ-secretase or the Aβ catabolism (Mastrangelo et al., 2005). In consequence, the increase in the Aβ production, observed by the presence of hPS1M146L in our tg model, could reflect either a gain-of-function due to the mutation itself or, more probably, an indirect effect of the PS1 mutations on the Aβ metabolism at a different point of the γ-secretase activity. This latter hypothesis may also explain the "apparent gain-of-function" of the γ-secretase and the consistent increase in the plaque number observed in all PS1xAPP tg models described so far. Further experiments should be done to clarify this point.

Acknowledgments

This work was supported by grants SAF2002-03448 (J.V.), FIS03/0177 (D.R.), and FIS03/0214 (A.G.). C. Caballero, S. Jimenez, D. Baglietto-Vargas, and I. Moreno-Gonzalez were supported by fellowships from Ministerio de Educación y Ciencia, Junta de Andalucia and Fondo de Investigaciones Sanitarias, respectively.

References

Araujo F,Tan S,Ruano D,Schoemaker H,Benavides J,Vitorica J. 1996. Molecular and pharmacological characterization of native cortical gamma-aminobutyric acid(A) receptors containing both alpha(1) and alpha(3) subunits. *J Biol Chem* **271**: 27902–27911.

Blanchard V,Moussaoui S,Czech C,Touchet N,Bonici B,Planche M,Canton T,Jedidi I,Gohin M,Wirths O. 2003. Time sequence of maturation of dystrophic neurites associated with Aβ deposits in APP/PS1 transgenic mice. *Exp Neurol* **184**: 247–263.

Borchelt DR,Lee MK,Gonzales V,Slunt HH,Ratovitski T,Jenkins NA,Copeland NG,Price DL,Sisodia SS.2002. Accumulation of proteolytic fragments of mutant presenilin 1 and accelerated amyloid deposition are co-regulated in transgenic mice. *Neurobiol Aging* **23**: 171–177.

Cai D,Netzer WJ,Zhong M,Lin Y,Du G,Frohman M,Foster DA,Sisodia SS,Xu H,Gorelick FS,Greengard P. 2006. Presenilin-1 uses phospholipase D1 as a negative regulator of beta-amyloid formation.*Proc Natl Acad Sci U S A* **103**: 1941–1946.

Campbell WA,Iskandar MK,Reed MLO,Xia W. 2002. Endoproteolysis of presenilin in vitro: inhibition by γ-secretase inhibitors. *Biochem.* **41**: 3372–3379

Chen F,Hasegawa H,Schmitt-Ulms G,Kawarai T,Bohm C,Katayama T,Gu Y,Sanjo N,Glista M,Rogaeva E,Wakutani Y,Pardossi-Piquard R,Ruan X,Tandon A,Checler F,Marambaud P,Hansen K,Westaway D,George-Hyslop P,Fraser P. 2006. TMP21 is a presenilin complex component that modulates γ-secretase but not epsilon-secretase activity. *Nature* **440**: 1208–1212.

Dewachter I,Van Dorpe J,Smeijers L,Gilis M,Kuiperi K,Laenen I,Caluwaerts N,Moechars D,Checler F,Vanderstichele H,Van Leuven F. 2000. Aging increased amyloid peptide and caused amyloid plaques in brain of old APP/V717I transgenic mice by a different mechanism than mutant presenilin1. *J Neurosci* **20**: 6452–6458.

Doglio LE,Kanwar R,Jackson GR,Perez M,Avila J,Dingwall C,Dotti CG,Fortini ME,Feiguin F. 2006.gamma-Cleavage-independent functions of presenilin, nicastrin, and Aph-1 regulate cell-junction organization and prevent Tau toxicity In vivo. *Neuron* **50**: 359–375.

Edbauer D,Winkler E,Regula JT,Pesold B,Steiner H,Haass C. 2003 Reconstitution of γ-secretase activity. *Nat Cell Biol* **5**: 486–488.

Hardy J,Selkoe DJ. 2002. The amyloid hypothesis of Alzheimer's disease: progress and problems on the road to therapeutics. *Science* **297**: 353–356.

Iwata N,Tsubuki S,Takaki Y,Shirotani K,Lu B,Gerard NP,Gerard C,Hama E,Lee HJ,Saido TC. 2001.Metabolic regulation of brain Aβ by neprilysin. *Science* **292**: 1550–1552.

Kakuda N,Funamoto S,Yagishita S,Takami M,Osawa S,Dohmae N,Ihara Y. 2006. Equimolar production of amyloid beta-protein and amyloid precursor protein intracellular domain from beta-carboxyl-terminal fragment by γ-secretase. *J Biol Chem* **281**: 14776–14786.

Kimberly WT,LaVoie MJ,Ostaszewski BL,Ye W,Wolfe MS,Selkoe DJ. 2003. γ-secretase is a membrane protein complex comprised of presenilin, nicastrin, aph-1, and pen-2. *Proc Natl Acad Sci U S A* **100**:6382–6387.

Lee MK,Borchelt DR,Kim G,Thanikaran G,Slunt HH,Ratovitski T,Martin LJ,Kittur A,Gandy S,Levey AI,Jenkins N,Copeland N,Price DL,Sisodia SS. 1997. Hyperaccumulation of FAD-linked presenilin 1 variants in vivo. *Nat Med* **3**: 756–760.

Leissring MA,Farris W,Chang AY,Walsh DM,Wu X,Sun X,Frosch MP,Selkoe DJ. 2003. Enhanced proteolysis of beta-amyloid in APP transgenic mice prevents plaque formation, secondary pathology, and premature death. *Neuron* **40**: 1087–1093.

Lewis HD,Beher D,Smith D,Hewson L,Cookson N,Reynolds DS,Dawson GR,Jiang M,Van der Ploeg LHT,Qian S. 2004. Novel aspects of accumulation dynamics and Aβ composition in transgenic models of AD. *Neurobiol Aging* **25**: 1175–1185.

Li YM,Lai MT,Xu M,Huang Q,DiMuzio-Mower J,Sardana MK,Shi XP,Yin KC,Shafer JA,Gardell SJ. 2000.Presenilin 1 is linked with gamma-secretase activity in the detergent solubilized state. *Proc Natl Acad Sci U S A* **97**: 6138–6143.

Lowry OH,Rosebrough NJ,Farr AL,Randall RJ. 1951. Protein measurement with the Folin phenol reagent. *J Biol Chem* **193**: 265–275.

Mastrangelo P,Mathews PM,Chishti MA,Schmidt SD,Gu Y,Yang J,Mazzella MJ,Coomaraswamy J,Horne P,Strome B,Pelly H,Levesque G,Ebeling C,Jiang Y,Nixon RA,Rozmahel R,Fraser PE,George-Hyslop P,Carlson GA,Westaway D. 2005. Dissociated phenotypes in presenilin transgenic mice define functionally distinct γ-secretases. *Proc Natl Acad Sci U S A* **102**: 8972–8977.

Mirnics K,Korade Z,Arion D,Lazarov O,Unger T,Macioce M,Sabatini M,Terrano D,Douglass KC,Schor NF,Sisodia S. 2005. Presenilin-1-dependent transcriptome changes. *J Neurosci* **25**: 1571–1578

Pardossi-Piquard R,Petit A,Kawarai T,Sunyach C,Alves da Costa C,Vincent B,Ring S,D'Adamio L,Shen J,Muller U. 2005. Presenilin-dependent transcriptional control of the Aβ-degrading enzyme neprilysin by intracellular domains of betaAPP and APLP. *Neuron* **46**: 541–554.

Price DL,Tanzi RE,Borchelt DR,Sisodia SS. 1998. Alzheimer's disease: genetic studies and transgenic models. *Ann Rev Genet* **32**: 461–493.

Ramos B,Baglietto-Vargas D,Rio JCd,Moreno-Gonzalez I,Santa-Maria C,Jimenez S,Caballero C,Lopez-Tellez JF,Khan ZU,Ruano D,Gutierrez A,Vitorica J. 2006. Early neuropathology of somatostatin/NPY GABAergic cells in the hippocampus of a PS1 x APP transgenic model of Alzheimer's disease. *Neurobiol Aging* **27**: 1658–1672.

Schmitz C,Rutten BPF,Pielen A,Schafer S,Wirths O,Tremp G,Czech C,Blanchard V,Multhaup G,Rezaie P,Korr H,Steinbusch HWM,Pradier L,Bayer TA. 2004. Hippocampal neuron loss exceeds amyloid plaque load in a transgenic mouse model of Alzheimer's disease. *Am J Pathol* **164**: 1495–1502.

Selkoe DJ. 2002. Alzheimer's disease is a synaptic failure. *Science* **298**: 789–791.

Terro F,Czech C,Esclaire F,Elyaman W,Yardin C,Baclet M-C, Touchet N,Tremp G,Pradier L,Hugon J.2002. Neurons overexpressing mutant Presenilin-1 are more sensitive to apoptosis induced by endoplasmic reticulum-golgi stress. *J Neurosci Res* **69**: 530–539.

Thinakaran G,Borchelt DR,Lee MK,Slunt HH,Spitzer L,Kim G,Ratovitsky T,Davenport F,Nordstedt C,Seeger M. 1996. Endoproteolysis of presenilin 1 and accumulation of processed derivatives in vivo. *Neuron* **17**: 181–190.

Unger T,Korade Z,Lazarov O,Terrano D,Schor NF,Sisodia SS,Mirnics K. 2005. Transcriptome differences between the frontal cortex and hippocampus of wild-type and humanized presenilin-1 transgenic mice. *Am J Psychiatry* **13**: 1041–1051.

Walsh DM,Klyubin I,Fadeeva JV,Cullen WK,Anwyl R,Wolfe MS,Rowan MJ,Selkoe DJ. 2002. Naturally secreted oligomers of amyloid beta protein potently inhibit hippocampal long-term potentiation in vivo. *Nature* **416**: 535–539.

Wang R,Wang B,He W,Zheng H. 2006. Wild-type presenilin 1 protects against Alzheimer's disease mutation-induced amyloid pathology. *J Biol Chem* **281**: 15330–15336.

West MJ,Coleman PD,Flood DG,Troncoso JC. 1994. Differences in the pattern of hippocampal neuronal loss in normal ageing and Alzheimer's disease. *Lancet* **344**: 769–772.

West MJ,Kawas CH,Stewart WF,Rudow GL,Troncoso JC. 2004. Hippocampal neurons in pre-clinical Alzheimer's disease. *Neurobiol Aging* **25**: 1205–1212.

Figures legends

Figure. 1. Heterogeneity in the Aβ production in 6-month-old PS1xAPP tg mice as shown by Western ELISA and immunohistochemistry. A, B: The Aβ content was determined by Western blots (using the mAb 6E10) in protein samples from different 6-month-old hippocampus (A) and cortex (B). The Western blots are representative of at least three replicates with different sample distribution. The protein loading between the different samples was tested by re-probing of the same Westerns using anti-β-actin (A,B, **lower panels**). No apparent inter-individual differences were observed. **C:** Quantitative analysis of the different Western blots showing the high variability between the different samples. The signal of the different samples was normalized by the corresponding expression of the β-actin. To avoid possible differences in exposure time between the different samples or other potential pitfalls two constant samples (Mice 233 and 15) were included in each blot. **D:** Plot of the Aβ content, determined in hippocampus and cortex, of each individual PS1xAPP mouse. As shown, a significant linear correlation could be established between both brain areas. **E:** Heterogeneity was also observed by ELISA quantification of total and Aβ1-42 from the same hippocampal samples. **F, G:** Aβ deposition was also determined by immunohistochemistry (using 6E10) in seven different 6-month-old PS1xAPP tg mice.

The amount of Aβ deposits was also heterogeneous as shown here for these two mice with low (**upper panel**) and high (**lower panel**) Aβ expression. The quantitative analysis of the plaque loading (G) also showed this high inter-individual variability between the different tg mice. Scale bar = 230 μm.

Figure 2. The heterogeneity in the Aβ production was independent of the APP and C99 levels and could reflect the variable expression of the tg PS1M146L. A: Representative Western blot showing the APP, C99, and Aβ peptides. Western blots were stained using the mAb 6E10. As shown, the variable levels of Aβ peptides were not reflected by modifications in either APP or C99 levels. **B:**Absence of inter-individual differences in the C99 fragments was confirmed with a polyclonal antibody against the C-terminal fragment of APP using an identical sample configuration as in (A). **C:** Quantitative analysis of C99 and Aβ the different Western blots shown (A). For APP quantification (**inset**), shorter exposure times were used. As shown, a low variability in APP and C99 expression was observed. **D:** Real time RT-PCR quantification of hPS1 (open symbols) and hAPP (closed symbols) expression in hippocampus (circles) and cortex (squares) of 6-month-old PS1xAPP mice. The expression of hPS1 was highly variable between the different samples. Please, note the different scale between hPS1 and hAPP. **E:** hPS1 mRNA expression level of hippocampus was plotted against the corresponding value obtained in cortex for each individual PS1xAPP mouse. As shown, a linear correlation was observed. **F:** Expression of Aβ peptides (data taken from Fig. 1C) seemed to be dependent on the expression of hPS1 (data taken from D). Note that data from both hippocampus and cortex could be fitted by the same linear relationship.

Figure 3. The highly variable expression of hPS1 was reflected in the generation of hCTF fragments, their competition with the corresponding endogenous mCTF and the production of Aβ peptides. A: Western blot analysis of the PS1 C-terminal fragments (CTFs) using the mAb MAB5232. As shown, the endogenous mCTF (**lanes 1,4**) was detected as a band of approximately 20 kDa whereas the corresponding hCTF (**lanes 2,3,5,6**) has a slightly lower mobility (approximately 22 kDa). A clear differential level of mCTF and hCTF could be observed between the different PS1xAPP mice. The PS1xAPP tg Mouse 15 (lane 5) displayed very low levels of hPS1-CTF whereas, under the same conditions, Mouse 233 (lane 6) displayed high levels. **B:** Relative intensity of hCTF (calculated as % of total, mCTF + hCTF) was plotted against the Aβ production from the same PS1xAPP mice (data taken from Fig. 1). As shown, a significant linear relationship could be established between these two parameters. **C:** Total (m + h) PS1-CTF slightly increased in the different PS1xAPP tg mice. The quantitative analysis of hCTF from three independent experiments (using four to five different PS1xAPP mice per experiment; represented by different symbols) were plotted against the total m + hCTF fragments. A clear saturation profile could be observed. **D:** When data from mCTF and hCTF were plotted, an apparent competition between both CTF fragments was observed. The data are from the same experiments as (C). **E:** Co-immunoprecipitation of PS1-CTF by anti-nicastrin polyclonal antibody. Solubilized hippocampal membranes

were immunoprecipitated by anti-nicastrin-Protein A-Sepharose complex or by Protein A-Sepharose (as negative control) and blotted using anti-PS1-CTF monoclonal antibody. A representative experiment of four different replicates with similar results is shown. Anti-nicastrin polyclonal antibody specifically immunoprecipitated a PS1-CTF band, Mr 22 kDa, similar to that observed in the solubilized membranes. This band was not present in absence of primary antibody. **D:** Quantitative analysis of the co-immunoprecipitated PS1-CTF. The results were normalized by the immunoprecipitated band observed in the WT mice and data are the mean ± SD of four different experiments.

Figure 4. The presence of the tg PS1M146L subunit enhanced the production of both Aβ total and 1-42. To determine, in vivo, the effect of the presence of PS1M146L in the production of Aβ peptides (total and 1-42), hemizygous PS1 and APP tg mice were crossed. The hippocampal and cortical Aβ content was analyzed by sandwich ELISA in all four genotypes (WT, PS1, APP, PS1xAPP) littermates of 6 months of age. No Aβ peptides were detected in WT or PS1 at this age. Aβ levels of APP and PS1xAPP tg mice are shown. In all cases, the Aβ, total and 1-42 increases significantly ($P < 0.05$) in the double PS1xAPP tg mice, as compared with APP littermates.

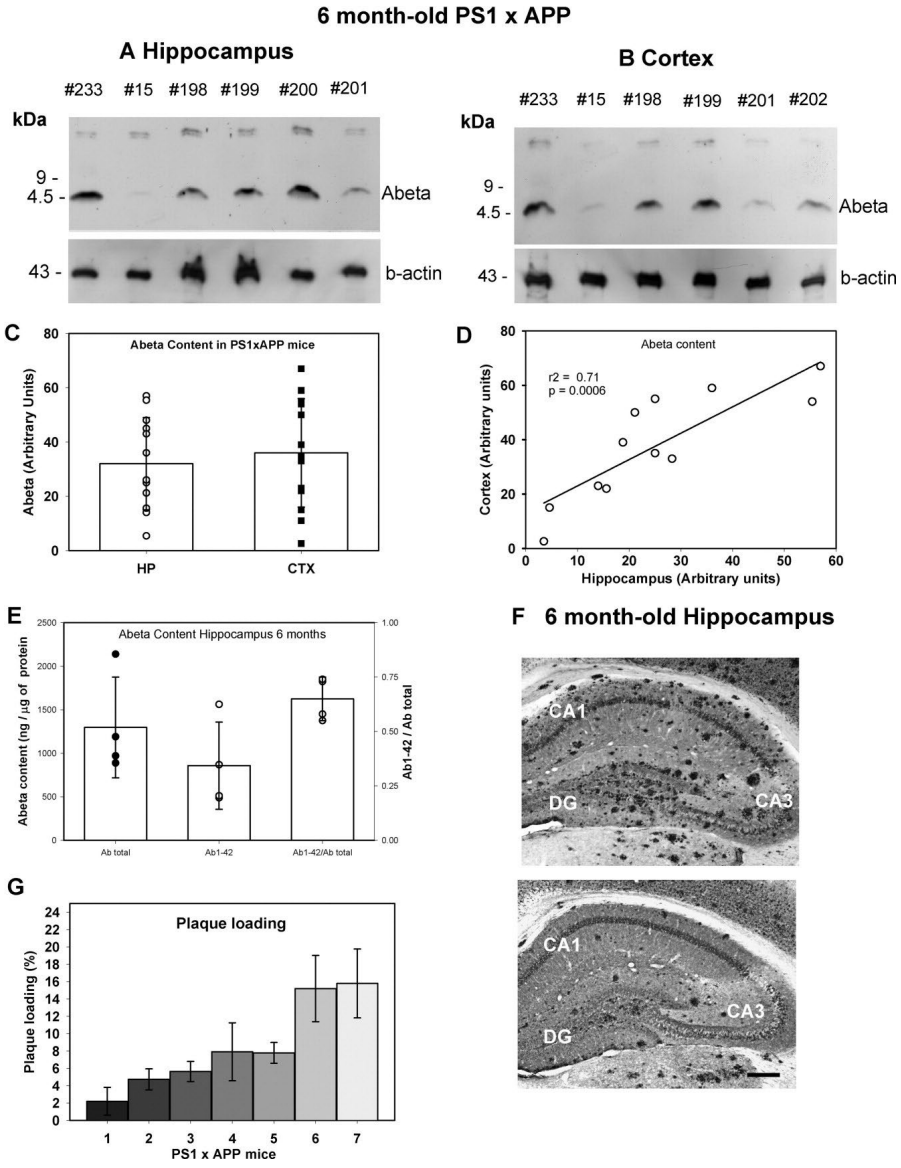
6 month-old PS1 x APP
A Hippocampus
#233 #15 #198 #199 #200 #201
kDa
9 -
4.5 -
Abeta
43 -
b-actin
B Cortex
#233 #15 #198 #199 #201 #202
kDa
9 -
4.5 -
Abeta
43 -
b-actin
C
Abeta Content in PS1xAPP mice
Abeta (Arbitrary Units)
HP
CTX
D
Abeta content
r2 = 0.71
p = 0.0006
Cortex (Arbitrary units)
Hippocampus (Arbitrary units)
E
Abeta Content Hippocampus 6 months
Abeta content (ng / µg of protein
Ab1-42 / Ab total
Ab total
Ab1-42
Ab1-42/Ab total
F 6 month-old Hippocampus
CA1
DG
CA3
CA1
CA3
DG
G
Plaque loading
Plaque loading (%)
PS1 x APP mice

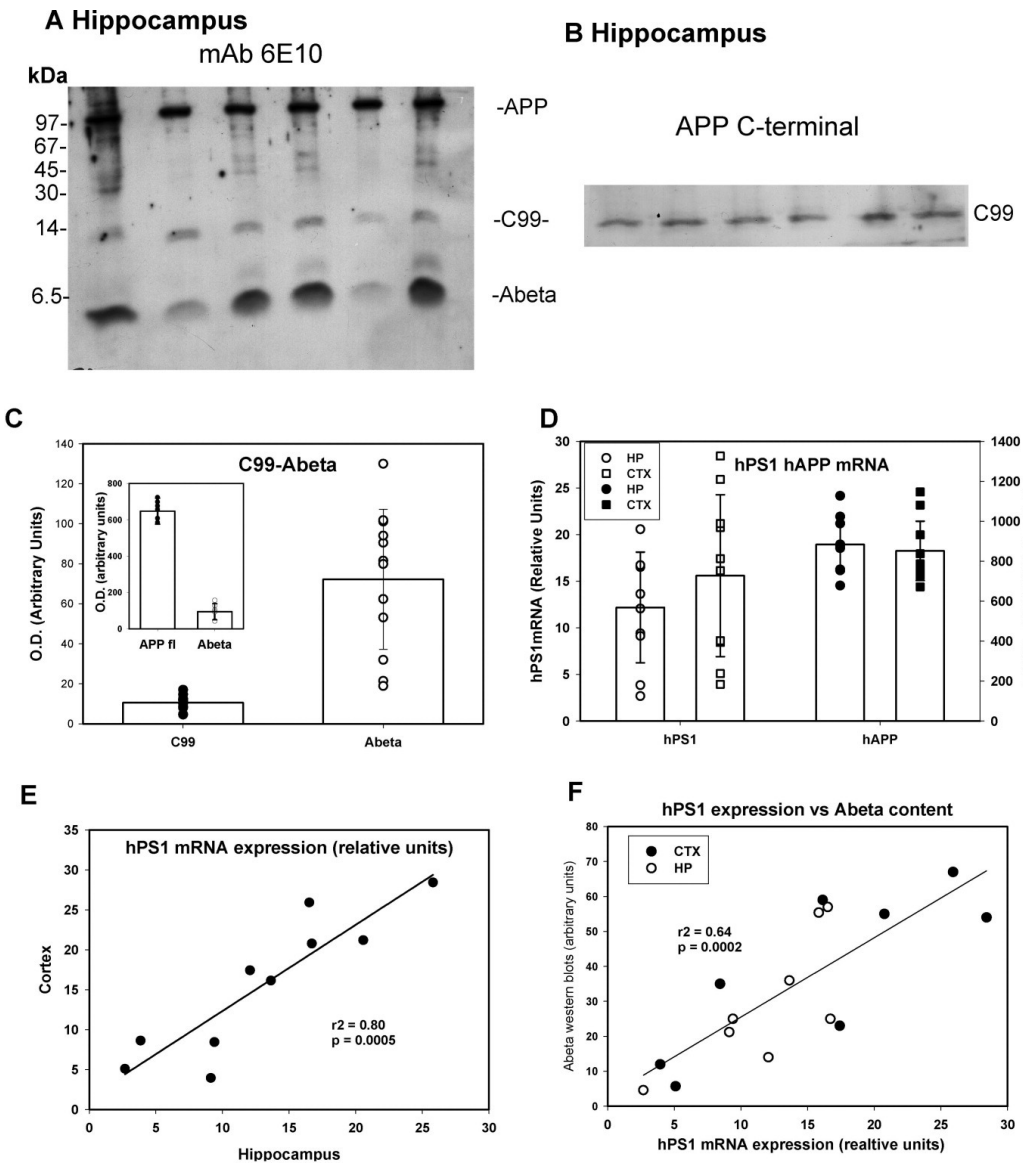
A Hippocampus
mAb 6E10
kDa
97-
67-
45-
30-
14-
6.5-
-APP
-C99-
-Abeta
B Hippocampus
APP C-terminal
C99
C
C99-Abeta
O.D. (Arbitrary Units)
O.D. (arbitrary units)
APP fl
Abeta
C99
Abeta
D
hPS1 hAPP mRNA
HP
CTX
HP
CTX
hPS1mRNA (Relative Units)
hAPP mRNA (Relative Units)
hPS1
hAPP
E
hPS1 mRNA expression (relative units)
Cortex
Hippocampus
r2 = 0.80
p = 0.0005
F
hPS1 expression vs Abeta content
CTX
HP
Abeta western blots (arbitrary units)
hPS1 mRNA expression (realtive units)
r2 = 0.64
p = 0.0002

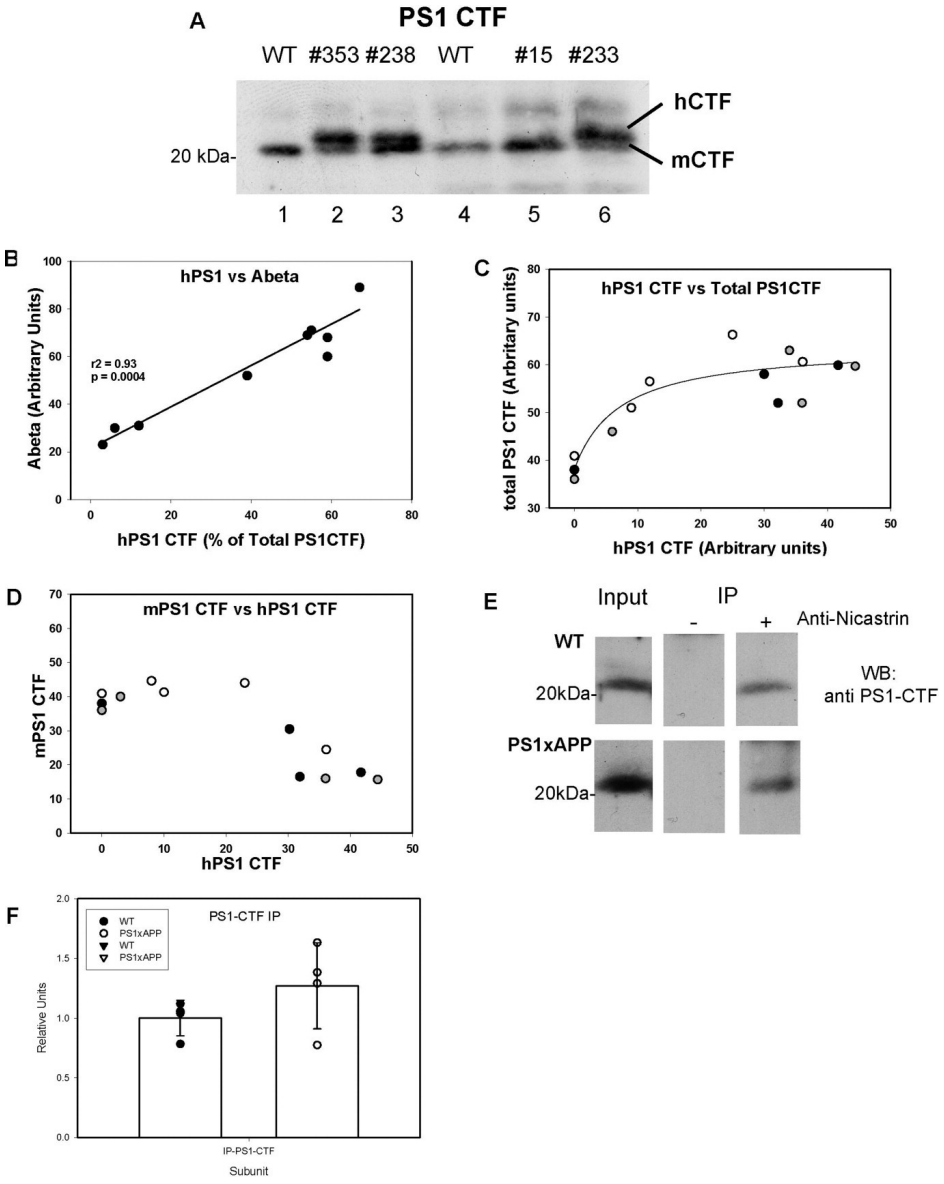
A
PS1 CTF
WT #353 #238 WT #15 #233
hCTF
mCTF
20 kDa-
1 2 3 4 5 6
B
hPS1 vs Abeta
r2 = 0.93
p = 0.0004
Abeta (Arbitrary Units)
hPS1 CTF (% of Total PS1CTF)
C
hPS1 CTF vs Total PS1CTF
total PS1 CTF (Arbitrary units)
hPS1 CTF (Arbitrary units)
D
mPS1 CTF vs hPS1 CTF
mPS1 CTF
hPS1 CTF
E
Input
IP
-
+
Anti-Nicastrin
WT
20kDa-
WB:
anti PS1-CTF
PS1xAPP
20kDa-
F
PS1-CTF IP
WT
PS1xAPP
WT
PS1xAPP
Relative Units
IP-PS1-CTF
Subunit

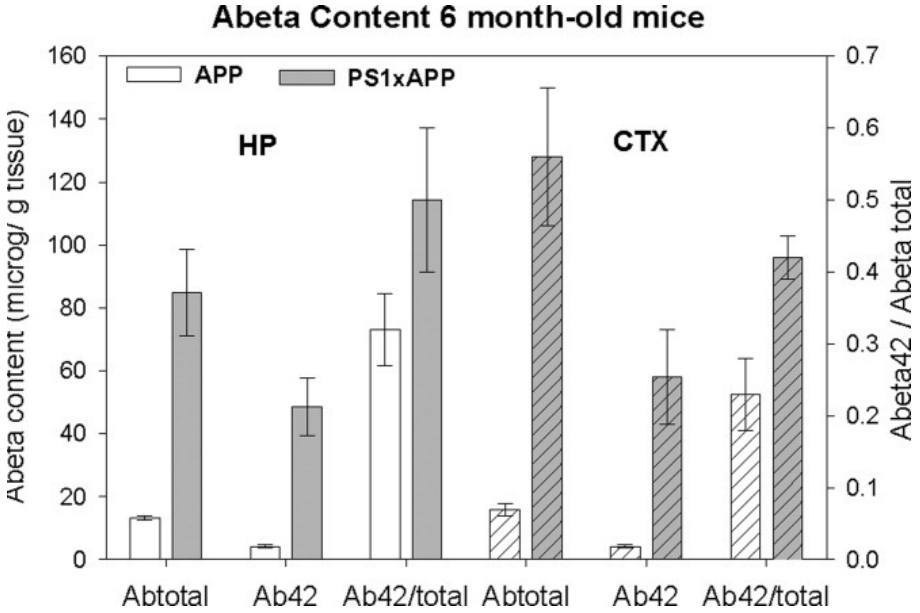
Abeta Content 6 month-old mice
APP
PS1xAPP
HP
CTX
Abeta content (microg/ g tissue)
Abeta42 / Abeta total
160
140
120
100
80
60
40
20
0
0.7
0.6
0.5
0.4
0.3
0.2
0.1
0.0
Abtotal
Ab42
Ab42/total
Abtotal
Ab42
Ab42/total